

# Quantum Hall Skyrmion Lattices at $g \approx 0$

Sumithra Sankararaman\* and R. Shankar†

*The Institute of Mathematical Sciences,  
C.I.T. Campus, Taramani, Chennai 600 113, India.*

(Dated: March 22, 2022)

## Abstract

We investigate the classical ground state configurations of a collection of skyrmions in the limit of vanishing L nd   $g$  factor. We show that in this limit, the skyrmions which are large and overlapping, behave qualitatively differently from small skyrmions. We investigate the system in various regimes of spin stiffness. We find that in all regimes, at  $g = 0$ , the ground state configuration is a rectangular skyrmion lattice with N el orientational ordering. The charge distribution has a higher symmetry of a face-centered rectangular lattice and the  $z$ -component of the spin polarization is zero. We also present general argument for the vanishing of spin polarization at  $g = 0$  at finite temperature and in the presence of disorder and discuss some experimental consequences of our results.

---

\* Email:sumithra@imsc.res.in

† Email:shankar@imsc.res.in

## I. INTRODUCTION

The lowest energy charged excitations about the  $\nu = 1$  ferromagnetic quantum Hall ground state are skyrmions. They are topological objects in which the spin gradually twists over an extended region. Their spin is greater than  $1/2$  and they carry an electric charge of  $\pm e$ . Skyrmions have a topological charge which equals their electric charge at  $\nu = 1$ <sup>1,2</sup>. Skyrmionic excitations are favoured over single particle excitations when the Landé g-factor is small i.e  $g \rightarrow 0$ <sup>1,3,4</sup>. Skyrmions which are produced around the  $\nu = 1$  ground state have been experimentally seen by in OPNMR and optical magneto-absorption experiments on Ga nuclei in an electron doped multiple quantum well structure<sup>5,6</sup>. A sharp fall in the spin polarisation of the 2D electron gas is seen on either side of  $\nu = 1$ , which indicates that a number of spins are being flipped by the addition or removal of a single electron, in contrast to single particle excitations where no extra spin is flipped. Small skyrmions have also been observed as low energy excitations about the  $\nu = 1$  state in tilted field measurements reported in<sup>7</sup>. The above experiments observe skyrmions where the number of flipped spins varies between 3 and 7. Low  $g$  experiments observe large skyrmions with a large number of flipped spins (50 and 36 respectively)<sup>8,9</sup>. In these experiments a low value of  $g$  is obtained either by suitably altering the stoichiometry while growing the sample or by application of hydrostatic pressure.

The low temperature ground state of a system of interacting skyrmions is expected to be a crystalline lattice<sup>10,11,12,13</sup>. Earlier calculations performed in the mean field limit by Brey *et. al.*<sup>10</sup> suggest that the ground state of a system of skyrmions is a square Skyrme crystal with an anti-ferromagnetic order in the planar component of the spin of the skyrmion. Later studies by Green *et. al.*, Rao *et. al.* and Timm *et. al.* analyze the classical ground state of the skyrmion lattice as  $\nu \rightarrow 1$  using the non-linear sigma model (NLSM)<sup>11,12,13</sup>. Green *et. al.* assume that the ground state is a triangular lattice with spiral ordering<sup>11</sup>. Rao *et. al.* report *triangle*  $\rightarrow$  *square*  $\rightarrow$  *triangle* transitions in the skyrmion lattice as a function of the filling factor near  $\nu = 1$  and at  $T=0$ <sup>12</sup>. Timm *et. al.* study a system of well separated skyrmions as described by an anti-ferromagnetic XY model and propose a  $T=0$  phase diagram in which the triangle and square phases are separated by Néel ordered, face-centered rectangular phases<sup>13</sup>. The classical and quantum phase transitions occurring in the Skyrme crystal has been studied using Hartree-Fock calculations by Côté *et. al.*<sup>14</sup>. Moon *et. al.* study the

renormalization effect of skyrmions and the thermodynamics of a skyrmion system, without assuming apriori lattice structures<sup>15</sup>.

At non-zero  $g$ , the charge and spin densities of skyrmions are peaked about its north pole if the vacuum spin polarization direction is taken to be the south pole. They fall off exponentially from their central value. The corresponding size is determined by the competition between the Coulomb repulsive energy and the Zeeman energy. The former favours an infinite size (power law fall-off) and the latter a zero size. The  $XY$  component of the skyrmion spin density assumes a "hedgehog" configuration. These configurations can be characterized by the orientation angle subtended between the position vector (with respect to the center of the skyrmion) and the  $XY$  component of the spin density at that point. The finite sized skyrmion therefore behaves like an oriented, charged disc. It is energetically favourable for nearby skyrmions to have opposite orientations. These considerations lead to small skyrmions being modeled by discs carrying an  $XY$  spin with coulomb repulsion and short range anti-ferromagnetic interactions<sup>13</sup>. The coulomb repulsion leads to a triangular lattice in the dilute limit and the  $XY$  antiferromagnetism in the orientational degree of freedom to the square lattice as the inter-skyrmion spacing decreases.

In this paper we show that this picture breaks down when the skyrmionic size is larger than the inter-skyrmion spacing. For instance, when  $g = 0$  there is no exponential damping and we show that the charge density is symmetric in the neighbourhood of the north and south poles. The oriented disc picture is then clearly invalid. We study the ground state configuration of a collection of skyrmions at  $g = 0$  and  $g = 0.05g_0$ , ( $g_0$  is the physical value of the Landé  $g$  factor). The energy of the system at  $g \approx 0$  is described well by the Non-linear Sigma Model energy functional<sup>16</sup>. We minimize this energy functional in three different regimes: (1) High stiffness regime in which the gradient term dominates the energy functional, (2) Low stiffness regime in which the Coulomb term dominates and (3) Intermediate stiffness in which both terms in the energy functional compete to generate a suitable ground state. Finally, we discuss the behaviour of the spin polarisation and its experimental consequences.

The rest of the paper is organised as follows. Section II, describes the NLSM energy functional. Section III discusses the ansatz used to solve the energy functional and the symmetries of that ansatz. In Section IV we discuss the minimum energy configuration in the high stiffness ,low stiffness and intermediate stiffness regimes. Section V we describe

a general argument for the vanishing of the spin polarization at  $g = 0$  and discuss the experimental consequences. Finally, the conclusions of this paper and a summary of the results is presented in Section VI.

## II. MODEL AND NLSM ENERGY FUNCTIONAL

We consider skyrmionic excitations about the  $\nu = 1$  ground state. The number density of skyrmions is given by  $n_{sky} = \frac{1-\nu}{\nu}n_c$ , where  $n_c$  is the carrier density. In our calculations we use the carrier density,  $n_c = 1.5 \times 10^{11} \text{ cm}^{-2}$  and change  $\nu$  by tilting the magnetic field. We localize the skyrmion centers on the lattice points of a Bravais lattice shown in Fig. 1. We choose a skyrmion density ( $n_{sky}$ ) of 1 skyrmion per unit cell (i.e one skyrmion per lattice point).

We measure all lengths in units of the magnetic length  $l_c = \sqrt{\frac{\hbar}{eB}}$  and all energies in terms of the cyclotron energy  $\hbar\omega_c$ , where  $\omega_c = (eB/m^*c)$ ,  $m^*$  is the effective mass of the electron. The area of the unit cell is fixed by the filling factor and is given by

$$A_{\square} = \frac{1}{n_{sky}} = \frac{2\pi}{1-\nu} \quad (2.1)$$

The local spin polarisation which is represented by unit vector field  $\mathbf{n}(\mathbf{x})$  is stereographically projected onto the complex plane by the transformation  $w = \cot(\theta/2)e^{i\phi}$ , where  $\theta$  and  $\phi$  are the polar angles of the spin vector  $\mathbf{n}(\mathbf{x})$ . In the rest of the paper we will work with the planar spin variable  $w$ .

The topological charge density is given by

$$\begin{aligned} \rho(\mathbf{x}) &= \frac{1}{4\pi} \epsilon_{ij} \mathbf{n} \cdot (\partial_i \mathbf{n} \times \partial_j \mathbf{n}) \\ &= \frac{\epsilon_{ij} \partial_i w \partial_j \bar{w}}{2\pi i (1 + w\bar{w})^2} \end{aligned} \quad (2.2)$$

The topological charge,  $Q(\mathbf{x}) = \int_{\square} d^2x \rho(\mathbf{x}) = 1$  ( $\int_{\square}$  denotes integration over the unit cell).

The low energy, long wavelength excitations about the  $\nu = 1$  ground state are described by the NLSM. The NLSM energy functional has to be minimized for different filling factors to get the minimum energy configurations of this lattice. The NLSM energy functional with Zeeman and Coulomb interactions is<sup>1,11,12</sup>:

$$E = E_{grn} + E_z + E_{coul} \quad (2.3)$$

The gradient or the spin exchange term proportional to  $\int d^2x |\partial_i \mathbf{n}(\mathbf{x})|^2$ , ( $i = x, y$ ), is calculated as

$$E_{grn} = \frac{\gamma}{2} \int_{\square} d^2x \frac{(\partial_x w \partial_x \bar{w} + \partial_y w \partial_y \bar{w})}{(1 + w \bar{w})^2} \quad (2.4)$$

where  $\gamma = \frac{e^*}{16\sqrt{2}\pi}$ . The gradient energy density is  $E_{grn}/A_{\square}$ , where  $A_{\square}$  is the area of the unit cell. This term alone is the pure NLSM and it has exact scale invariant solutions<sup>17</sup>.

The Zeeman term is proportional to the z-component of the total spin i.e. to  $\frac{\nu}{2\pi} \int_{\square} d^2x \frac{(1+n^z)}{2}$  (where  $n^z$  is the z-component of  $\mathbf{n}(\mathbf{x})$ ). In our units the average number of electrons is  $\frac{\nu}{2\pi}$ . The z-component of the total spin is

$$(Total \ spin)_z = \frac{\nu}{2\pi} \int_{\square} d^2x \frac{\bar{w}w}{(1 + \bar{w}w)} \quad (2.5)$$

Therefore,

$$E_z = g^* \frac{\nu}{2\pi} \int_{\square} d^2x \frac{\bar{w}w}{(1 + \bar{w}w)} \quad (2.6)$$

where  $g^* = \frac{g\mu_B B}{\hbar\omega_c}$ . The Zeeman energy density is therefore  $E_z/A_{\square}$ , where  $A_{\square}$  is the area of the unit cell.

The Coulomb energy density term is a term of the form

$$E_{coul} = \frac{e^*}{2} \frac{1}{A_{tot}} \int_{\mathbf{x}, \mathbf{y}} \rho(\mathbf{x}) \frac{1}{|\mathbf{x} - \mathbf{y}|} \rho(\mathbf{y}) \quad (2.7)$$

where  $e^* = (e^2/Kl_c)(1/\hbar\omega_c)$  and  $A_{tot}$  is the total area of the lattice.

The Coulomb term arises because the electric charge density is proportional to the topological charge density. Since the topological charge density explicitly appears in the above expression the spin orientation gets automatically tied to the Coulomb energy. The four dimensional integral in the Coulomb term can be converted to a sum over the reciprocal lattice.

$$\begin{aligned} E_{coul} &= \frac{1}{A_{\square}} \sum_{\{\mathbf{R}\}} \int_{\mathbf{x}, \mathbf{y} \in \square} \rho(\mathbf{x}) \frac{1}{|\mathbf{x} - \mathbf{y} + \mathbf{R}|} \rho(\mathbf{y}) \\ &= \frac{1}{A_{\square}} \sum_{\mathbf{R}} \int \frac{d^2g}{(2\pi)^2} e^{i\mathbf{g} \cdot \mathbf{R}} |\tilde{\rho}(\mathbf{g})|^2 \frac{2\pi}{|\mathbf{g}|} \end{aligned} \quad (2.8)$$

After doing the summation over  $\{\mathbf{R}\}$  and converting the integral over  $\mathbf{g}$  to a sum we get

$$E_{coul} = \frac{e^* \pi}{A_{\square}^2} \sum_{\{\mathbf{G}_R\}} |\tilde{\rho}(\mathbf{G}_R)|^2 \frac{1}{|\mathbf{G}_R|} \quad (2.9)$$

where  $\tilde{\rho}(\mathbf{G}_R) = \int_{\mathbf{x} \in \square} \rho(\mathbf{x}) e^{i\mathbf{G}_R \cdot \mathbf{x}}$ ,  $\mathbf{G}_R$  lies in the reciprocal lattice and  $A_{\square}$  is the area of the unit cell.

### III. ANSATZ AND SYMMETRIES

In this section we will describe and motivate the ansatz we will use to minimise the energy functional discussed above. Let us first consider the model without the Coulomb and Zeeman interactions. In this case it is known<sup>17</sup> that any meromorphic function  $w(z)$  is an exact solution of the equations of motion. Since the positions of the poles and zeros define a meromorphic function upto a multiplicative constant, the most general  $N$  skyrmion solution can be written as,

$$w_0(z) = w_\infty \frac{\prod_{m=1}^N (z - \bar{\mathbf{R}}_m)}{\prod_{n=1}^N (z - \mathbf{R}_n)} \quad (3.1)$$

$w_\infty$  specifies the direction of the spin polarization at  $|z| \rightarrow \infty$ . Equation (3.1) can be rewritten as,

$$w_0(z) = w_\infty + \sum_{n=1}^N \frac{\lambda_n}{(z - \mathbf{R}_n)} \quad (3.2)$$

$\lambda_n$  are  $N$  complex numbers which are given by the solution of the  $N$  linear equations,

$$w_\infty + \sum_{n=1}^N \frac{\lambda_n}{\bar{\mathbf{R}}_m - \mathbf{R}_n} = 0 \quad (3.3)$$

If we choose  $w_\infty = 0$ , corresponding to the spin polarization at infinity pointing in the  $-\hat{z}$  direction, and take the  $N \rightarrow \infty$  limit, equation (3.1) is written as,

$$w_0(z) = \sum_{\mathbf{R}} \frac{\lambda(\mathbf{R})}{(z - \mathbf{R})} \quad (3.4)$$

This motivates an ansatz of the form

$$w(z) = w_0(z)F(z) \quad (3.5)$$

for the fully interacting model. The skyrmion lattice is obtained by letting  $\{\mathbf{R}\}$  go over the position vectors of a lattice. For a Bravais lattice with basis vectors  $e_1$  and  $e_2$ ,  $\mathbf{R} = ne_1 + me_2$ , where  $n$  and  $m$  are integers. Further when  $|e_1| = |e_2| = e$  these basis vectors describe a face-centered rectangular lattice as shown in Fig. 1. They subtend an angle  $\theta$  at the origin. When  $\theta = 2\pi/3$  the lattice is a triangular lattice. When  $\theta = \pi/2$  the lattice is rectangular with  $a$  and  $b$  as the length of its sides.  $a/b$  is the aspect ratio of the rectangle.  $a/b = 1$  corresponds to the special case of a square lattice.  $F(z)$  is a smooth, non-analytic

function with the periodicity of the lattice. For the rectangular lattice we take it to be of the form,

$$\begin{aligned} F(z) &= \frac{e^{-\kappa_{np}r_{np}}}{e^{-\kappa_{sp}r_{sp}}} \\ r_{np} &= \sqrt{\sin^2(\pi x/a) + \sin^2(\pi y/b)} \\ r_{sp} &= \sqrt{\cos^2(\pi x/a) + \cos^2(\pi y/b)} \end{aligned}$$

The spin configuration corresponding to this ansatz is quasi-periodic. We have,

$$w(z + \mathbf{R}) = e^{i\mathbf{q}\cdot\mathbf{R}}w(z) \quad (3.6)$$

i.e. the spin rotates about the  $z$ -axis by an angle  $\mathbf{q}\cdot\mathbf{R}$  when translated by  $\mathbf{R}$ . However the energy has the periodicity of the lattice (since all the energies depend on  $\bar{w}w$ ). As shown in earlier work<sup>12</sup>,  $w(z)$  describes a configuration with skyrmion number one per lattice site. The mapping  $w = \cot(\theta/2)e^{i\phi}$  implies that the anti-podal points  $\theta = 0$  and  $\theta = \pi$  correspond to the poles and zeroes of  $w_0(z)$ . In the rest of the paper, we will refer to the poles as the “north poles” and the zeroes as the “south poles” respectively.

If we take  $\kappa_{sp} = 0$  and  $1/\kappa_{np} \ll a, b$ , then the ansatz in equation (3.5) is essentially the same as the one used in<sup>12</sup>. The charge and spin densities are then concentrated about the north poles. In this regime, each skyrmion can be visualised as a charged, oriented disc. The orientation corresponding to the angle the  $XY$  component of the spin density at any point makes with the vector joining that point with the center of the disc. The ansatz in equation (3.5) then corresponds to a collection of well separated skyrmions centered at the lattice sites (see Fig. 1). The vector  $\mathbf{q}$  can be interpreted as specifying a spiral orientation order for these skyrmions. The orientation rotates by  $\mathbf{q}\cdot\mathbf{R}$  when we move by  $\mathbf{R}$ . This is the picture used in reference<sup>13</sup> and the classical phase diagram can be qualitatively understood in terms of the long range coulomb repulsion between the discs (which favours a triangular lattice) and a short range antiferro-orientational interactions (which prefer an unfrustrated square lattice). When  $g = -0.44$ , the value for  $GaAs$  at low pressures, previous theoretical and experimental work show that the skyrmions have a spin  $s \approx 5$ . The spin can be related to the rms charge radius as  $\langle r^2 \rangle = 2s$  (see Appendix 2). Skyrmions can be called small when this radius is smaller than half the lattice spacing  $\sqrt{\frac{2\pi}{(1-\nu)}}$ . Skyrmions of spin  $\approx 5$  have a size of  $\approx 3$ . At  $\nu = 0.9$ , the lattice spacing is around 8. The skyrmions are thus well separated at  $\nu \geq 0.9$ . The system of skyrmions in this regime is well described by the oriented, charged

disc picture. As  $g$  is decreased, the skyrmions become larger and, as we will show below, this picture breaks down.

We show plots of the spin density and charge density in a lattice of well separated skyrmions. Figures 2. and 3. show the XY spin configuration and the charge density in a triangular lattice of well separated skyrmions<sup>20</sup>. The spins are ordered into a triangular lattice (with ABC sub-lattice structure) with  $\mathbf{q} = (2\pi/3, 2\pi/3)$ . Figures 4. and 5. show the XY spin configuration and the charge density distribution for a square lattice of well separated skyrmions. The spins have Néel order (with AB sub-lattice structure) with  $\mathbf{q} = (\pi, \pi)$ . We notice that the charge is peaked only around the “north poles” (the lattice points).

Let us now consider the extreme case i.e.  $g = 0$ . We first look at the high stiffness limit i.e. when the coefficient of the gradient term,  $\gamma$  is large. The gradient energy then dominates the NLSM energy functional. This energy is exactly minimised by any analytic ansatz. So in this regime, we will be putting  $\kappa_{np} = \kappa_{sp} = 0$ . The ansatz is then  $w(z) = w_0(z)$  with  $\mathbf{q}$  and  $\lambda$  as the variational parameters. The energy minimization procedure and results will be described in the next section. Here we discuss some of the important features of the spin and charge density distributions corresponding to this ansatz.

Since there is exactly one skyrmion per unit cell, there is one north pole and one south pole per unit cell. From the form of  $w_0(z)$  given in equation (3.4), it is obvious that the north poles are at  $\{\mathbf{R}\}$ . As we will now show, for a given lattice,  $\mathbf{q}$  determines the positions of the south poles. First consider a system of two skyrmions located at  $\mathbf{R}$  and  $-\mathbf{R}$ . This configuration is described by,

$$w(z) = \lambda \left( \frac{e^{i\mathbf{q}\cdot\mathbf{R}}}{z - \mathbf{R}} + \frac{e^{-i\mathbf{q}\cdot\mathbf{R}}}{z + \mathbf{R}} \right) \quad (3.7)$$

The zero of this ansatz is located at  $-i\mathbf{R}\tan(\mathbf{q}\cdot\mathbf{R})$ . Thus given the positions of the two skyrmions, the position of the zero is determined by  $\mathbf{q}$ .

We will now illustrate that the position of the zero is determined by the value of  $\mathbf{q}$  by considering the case of a face-centered rectangular lattice. These lattices are described by the basis vectors  $e_1$  and  $e_2$ . The unit cell is also shown. The center of the unit cell is located at  $z_0 = (e_1 + e_2)/2$ . Let us first consider Néel order  $\mathbf{q} = (\pi, \pi)$ . Now,

$$w(z_0) = \sum_{nm} \frac{e^{i\pi(n+m)}}{(n - 1/2)e_1 + (m - 1/2)e_2} \quad (3.8)$$

Reflecting every lattice point about the point  $z_0$  by the transformation  $n = -n' - 1$  and



$m = m' - 1$ , we can show that the above equation becomes

$$\begin{aligned} w(z_0) &= \sum_{n'm'} \frac{e^{i\pi(n'+m')}}{(-n' + 1/2)e1 + (-m' + 1/2)e2} \\ &= -w(z_0) \end{aligned} \quad (3.9)$$

which implies  $w(z_0) = 0$ . Hence the point  $z_0$  which is the center of the unit cell of the Bravais lattice is the location of the zero of the ansatz or the south pole. We note here that the point  $z_0 = (e1 + e2)/2$  is the south pole independent of specific values of  $e1$  and  $e2$  as long as there is Néel order. Hence in a triangular lattice and a rectangular lattice the south pole will lie at the center of the unit cell when these lattices are Néel ordered.

Now consider a triangular lattice with  $\mathbf{q} = (2\pi/3, 2\pi/3)$  ordering. We will now show that the position of the zero lies at the point  $c_0 = (e1 - e2)/3$ . A rotation of a lattice point  $\mathbf{R}$  about this point through an angle of  $2\pi/3$  takes it to a point  $\mathbf{R}'$  which also lies on the lattice. We know,

$$w(c_0) = \sum_{nm} \frac{e^{i2\pi/3(n+m)}}{(c_0 - \mathbf{R})} \quad (3.10)$$

On multiplying  $e^{i2\pi/3}$  to the numerator and denominator of  $w(c_0)$  it becomes

$$w(c_0) = e^{i2\pi/3} \sum_{n'm'} \frac{e^{i2\pi/3(n'+m')}}{(c_0 - \mathbf{R}')} \quad (3.11)$$

Since  $\mathbf{R}'$  is also a Bravais lattice vector

$$w(c_0) = e^{i2\pi/3} w(c_0). \quad (3.12)$$

Hence, we find that  $c_0 = (e1 - e2)/3$  is the south pole of the ansatz for a triangular lattice with  $(2\pi/3, 2\pi/3)$  order.

When the ordering on a triangular lattice changes from Néel  $(\pi, \pi)$  to  $(2\pi/3, 2\pi/3)$ , the position of the south pole moves from  $z_0 = (e1 + e2)/2$  to the point  $c_0 = (e1 - e2)/3$ . Hence we see that the position of the south pole of the ansatz on a fixed lattice is controlled by the parameter  $\mathbf{q}$ . In the rest of this section we will consider a rectangular lattice with Néel order and an aspect ratio of  $a/b$ . The south poles of the ansatz are located at the centers of the unit cells.

We will now study the properties of the ansatz on a rectangular lattice with Néel order. We show that there exists a special value of  $\lambda = \lambda_s$  at which the charge and spin densities

are symmetric about the north poles and south poles. This is true if the ansatz obeys the condition

$$w(z + (e1 + e2)/2) = \frac{1}{w(z)} \quad \text{at} \quad \lambda = \lambda_s \quad (3.13)$$

and hence the charge density and spin polarisation density are

$$\rho(w) = \frac{1}{2\pi i} \frac{\epsilon_{ij} \partial_i w \partial_j \bar{w}}{(1+w\bar{w})^2} = \rho(1/w) \quad (3.14)$$

$$s_z(w) = \frac{1}{2\pi} \frac{1-w\bar{w}}{1+w\bar{w}} = -s_z(1/w)$$

Thus, if Eq. 3.13 is true, the charge density is symmetric near the north and south poles and the spin is also symmetric but in opposite directions near these poles.

We impose the condition in Eq. (3.13) close to the north and south poles and obtain an equation for  $\lambda_s$  as follows. Expanding  $w(z = z_{np} + \epsilon)$  about the north pole ( $z_{np}$ ) we find that to leading order  $w(z) = \frac{\lambda}{\epsilon}$ . Expanding about the position of the south pole  $z_0 = (e1 + e2)/2$  we get

$$\begin{aligned} w(z) &= w(z_0) + \epsilon \partial_z w(z) \Big|_{z_0} \\ &= \epsilon \sum_{n_1, n_2} \frac{\lambda (-1)^{n_1 + n_2}}{(z_0 - (n_1 e1 + n_2 e2))^2}. \end{aligned} \quad (3.15)$$

The condition in Eq. 3.13 means that  $\lambda_s$  obeys

$$\frac{1}{\lambda_s^2} = \sum_{n_1, n_2} \frac{(-1)^{n_1 + n_2}}{(z_0 - (n_1 e1 + n_2 e2))^2}. \quad (3.16)$$

This was solved for numerically for  $\lambda_s$  and the condition in Eq. 3.13 was checked for all  $z$ . For example, for a Néel ordered rectangular lattice with an aspect ratio of  $\sqrt{3}$ ,  $\lambda_s$  was numerically calculated to be equal to 8.42. Even though the  $\lambda_s$  was obtained by imposing Eq. 3.13 at points close to the north and south poles, the numerical calculation described above shows that Eq. 3.13 is satisfied at all  $z$ . Thus at  $\lambda_s$  the charge and spin densities are symmetric about the north and south poles.

Having shown that at a particular value of  $\lambda = \lambda_s$  the charge and spin densities are symmetric around the north and south poles of a rectangular lattice with Néel order, we motivate some more properties of this configuration which will be numerically verified in the next section. For such a rectangular lattice with an aspect ratio of  $\sqrt{3}$ , the north poles

and south poles form a smaller triangular lattice. At the value  $\lambda = \lambda_s$ , the charge and spin density also have the symmetry of this smaller triangular lattice since they are symmetric about the north and south poles (see fig. 3). Since such a configuration corresponds to a charge distribution with the triangular lattice symmetry we expect that the Coulomb energy will be minimised for such a distribution. For the special case of the square lattice with aspect ratio 1, the charge and spin densities also have the symmetry of a smaller square lattice at the value  $\lambda_s$ . This is our motivation for minimising the variational ansatz for  $w(z)$  with the variational parameters as  $\theta$ ,  $q$ ,  $\lambda$  and aspect ratio. We do this calculation numerically to find the optimum value for these parameters in the lowest energy configuration.

In order to contrast the behaviour of spin and charge density for overlapping, large skyrmions with that of well separated, small skyrmions we plot the XY spin configurations and charge density profiles for a lattice of overlapping skyrmions. Figures 6. and 7. show these plots for a rectangular lattice with an aspect ratio of  $\sqrt{3}$ . We see that the XY spin configuration is very different from that shown in Figure 2. Also, the charge orders into a honeycomb lattice which has the symmetry of a triangular lattice. Figures. 8. and 9. show the plots for a square lattice of overlapping skyrmions.

We note here that the above features of the analytic ansatz remain true for a general ansatz  $w(z) = w_0(z)F(z)$  as long as  $F(z)$  is a function that respects the north pole-south pole symmetry. We discuss below a certain type of such functions and also conditions under which the north pole- south pole symmetry is broken.

In the low and intermediate stiffness regimes the gradient term does not dominate the energy functional anymore. Hence the requirement of the analyticity of the ansatz is not valid any longer. The ansatz can have an exponential cut-off via the function  $F(z)$ . In view of the north pole-south pole symmetry (which is still valid at  $g = 0$ ), we choose to damp the ansatz around the north and south pole in a symmetric way. Accordingly we choose,  $\kappa_{np} = \kappa_{sp}$  in Eq. (3.6). This form for  $F(z)$  preserves the north pole-south pole symmetry.

Symmetry about the north and south poles can be broken in two ways. One way is by choosing the scale  $\lambda$  to be different from the symmetric value  $\lambda_s$  thus making the charge and spin densities asymmetric about the north and south poles. The other way is to use different exponential cut-off scales around both poles (*i.e*  $\kappa_{np} \neq \kappa_{sp}$ ). This can be accomplished by

$$F(z) = \frac{e^{-\kappa_1 r_{np}}}{e^{-\kappa_2 r_{sp}}} \quad (3.17)$$

Such an asymmetry can be induced by a large value of  $g$ . In the extreme case when the cut-offs are such that the charge is peaked entirely around the north pole, the overlap is very small and the oriented disc picture is valid.

#### IV. ENERGY MINIMISATION : GROUND STATE CONFIGURATIONS

In this section we show that the special value  $\lambda_s$  at which the north and south poles are symmetric is the one at which the energy is minimised. We also show below that in the minimum energy configuration the charge density has the symmetry of a triangular lattice in the high stiffness limit and that of a square lattice in the low stiffness limit. This corresponds to the skyrmion lattice being rectangular with an aspect ratio of  $\sqrt{3}$  in the former case and square in the later case. In intermediate stiffness regimes, the aspect ratio interpolates between  $\sqrt{3}$  and 1. At the minimum, the spin density is peaked equally in opposite directions at the north and south poles which means  $\langle s_z \rangle = 0$  in the unit cell. The vanishing of the  $z$ -component of the spin the unit cell at  $\lambda = \lambda_s$  is a universal feature of our calculations.

##### A. High Stiffness Regime

In this regime at  $g = 0$ , the NLSM energy functional has contributions from the gradient term and the Coulomb term. Since the coefficient multiplying the gradient term,  $\gamma$  (the spin stiffness), is large the gradient energy dominates the energy functional. We minimize the energy functional with the analytic ansatz defined in the previous section. As mentioned earlier, this ansatz minimizes the gradient term exactly and hence is a good choice in the high stiffness limit. For large, overlapping skyrmions, we expect that the charge density has a higher symmetry than the underlying lattice. Based on the arguments in the previous section, we can see that this higher symmetry involves the symmetric distribution of charge and spin around the north and south poles. The charge density has the symmetry of a face-centered rectangular lattice if the underlying skyrmion lattice is rectangular.

We numerically minimize the NLSM energy functional with the ansatz for  $w(z)$  on a rectangular lattice with the quantities  $\mathbf{q}, \lambda$  and aspect ratio  $a/b$  as the variational parameters. Néel orientation order (*i. e.*  $\mathbf{q} = (\pi, \pi)$ ) is chosen by the minimum energy configuration.

This ensures that the south pole lies at the center of the rectangular unit cell. An aspect ratio of  $a/b = \sqrt{3}$  is chosen by the minimum energy configuration (see Fig. 10). At these values for  $\mathbf{q}$ ,  $a/b$  and  $\lambda = \lambda_{min}$  the charge density is symmetrically distributed around the north and south poles of the distribution as shown in Fig. 11. Hence this value of  $\lambda = \lambda_{min}$  is also the special value  $\lambda_s$  discussed in the previous section at which there is complete symmetry between the north and south poles. The charge density has the symmetry of a triangular lattice at this point.

The spin density peaks equally in opposite directions at the north pole and south pole. Hence the most symmetric distribution corresponds to a situation in which the total  $z$ -component of the spin is zero.

Because of the absence of the competing Zeeman term, there is no other length scale competing with the length scale of the Coulomb energy. The scaling relation is  $E_{coul}(\lambda, \mathbf{q}) = \frac{1}{\lambda} E_{coul}(1, \mathbf{q})$  (see Appendix 1). As the filling factor is varied, the length scale corresponding to the Coulomb energy changes. Thus, the length scale  $\lambda$  should scale with the filling factor (lattice spacing) but the ground state configuration does not change. If the energy is minimised at a certain filling factor (corresponding to lattice spacing  $e_1$ ) by a value  $\lambda_1$ , then the energy at another filling factor (corresponding to another lattice spacing  $e_2$ ) is minimised by a value  $\lambda_2$  such that  $\lambda_1/e_1 = \lambda_2/e_2$  is satisfied. This scaling of  $\lambda_{min}$  with the lattice parameter  $e$  is shown as  $\nu$  is changed (see Fig. 12). The ground state remains a rectangular lattice with aspect ratio of  $\sqrt{3}$  with Néel order for all filling factors at  $g = 0$ .

To conclude this subsection we give some details regarding the actual numerical minimization procedure used and some checks that were done. The numerical routine used was a downhill simplex routine in the three parameter space of  $\mathbf{q}$ ,  $\lambda$  and  $a/b$ . This routine minimized the energy functional with respect to the above parameters and returned the minimised value of energy at the appropriate values of these parameters. The minimization was carried out for many filling factors close to 1. As explained in Section II, different filling factors correspond to varying the area of the lattice. The numerical code was first checked to give the correct topological charge of 1 per unit cell (with an error of less than 0.1%). The vanishing of the  $z$ -component of the spin was numerically seen when  $\lambda = \lambda_{min}$ , lending support for our expectation of complete north pole-south pole symmetry at this point.

## B. Low and Intermediate Stiffness Regimes

We now consider the opposite limit (zero stiffness limit) at  $g = 0$  for a system of overlapping skyrmions. In this limit only the Coulomb energy contributes to the energy functional at  $g = 0$  and hence minimum energy configurations of the skyrmion lattice are determined by the minimum of the Coulomb energy. The Coulomb energy is minimized by a suitable configuration in which the charge is uniformly distributed. The ansatz used for the minimisation need not be analytic any longer and can have an exponential cut-off. Keeping in mind the north and south pole symmetry we chose to damp the ansatz around the north and south poles in a symmetric way. This is done by choosing  $F(z)$  to be a function with the periodicity of the north pole-south pole structure in the unit cell. The form for  $F(z)$  is given in Eq. (3.6) with  $\kappa_{np} = \kappa_{sp} = \kappa$ .

The energy is minimized with this ansatz on a Bravais lattice with respect to  $\mathbf{q}$ ,  $\lambda$ ,  $\kappa$  and aspect ratio  $a/b$ . We find that the ground state configuration is a square lattice with Néel order and  $s_z = 0$  (see Fig. 13). The type of lattice does not change with filling factor and the scaling of  $\lambda$  and Coulomb energy with lattice size is observed. The charge density has the symmetry of a square lattice. The spin density is also peaked in opposite directions at the north and south poles.

We have also checked whether an ansatz which describes a charge density with a different behaviour at small  $r$  will change the features described above. For this purpose we chose an ansatz

$$\begin{aligned} w(z) &= w_0(z)F(z) \\ F(z) &= \frac{e^{-\kappa_1 r_{np}} (1 + \kappa_2 r_{np})}{e^{-\kappa_1 r_{sp}} (1 + \kappa_2 r_{sp})} \end{aligned} \quad (4.1)$$

ensuring the symmetry of the north and south poles. When the minimization was done for this ansatz we find that Néel order and  $s_z = 0$  are still preferred with a square lattice as the ground state at all filling factors. At filling factors below  $\nu = 0.93$ , we find that  $\kappa_2 \ll \kappa_1$  and the charge density has the same behaviour as shown in Fig. 13. Between filling factors 0.93 and 0.98 we find that  $\kappa_2 > \kappa_1$  and the charge gets distributed to the lattice points as well as the center of the unit cell.

In the intermediate regime the stiffness is chosen to be at its physical value  $\gamma$ . All three terms (gradient energy, Zeeman energy and Coulomb energy) contribute to the energy

functional. The ansatz used in Eq. (3.5) is used to determine the ground state configuration at  $g = 0$ . We find that the minimum energy configuration is a rectangular lattice with an aspect ratio which is ansatz and filling factor dependent. However the spin configuration still has Néel order and  $s_z = 0$  for all these configurations.

## V. EXPERIMENTAL CONSEQUENCES

Our calculations predict two universal features of the  $g = 0$  system. (i) The skyrmion lattice is rectangular with Néel orientational order, (ii) the spin polarization is exactly zero. It is difficult to directly experimentally observe skyrmion lattices and no such experiments have been done so far. However the spin polarization can and has been measured using NMR and optical techniques at  $g = g_0^{5,6,18}$ .

Our calculations are done at zero temperature and in absence of disorder. However, disorder is always present in real systems and is crucial to the physics of plateau formation in quantum Hall systems. Thermal effects are also expected to be important at the temperatures ( $\sim 1K$ ) where the experiments are typically done. In fact theoretical<sup>11,13</sup> and experimental<sup>19</sup> evidence indicates that the skyrmion lattice would have melted at these temperatures. It is therefore important to consider the effects of thermal fluctuations and disorder before making predictions for experiments.

### A. Spin Polarization at $g = 0$

In this section, we present a general proof for the vanishing of the thermal average of the spin polarization at  $g = 0$  in the presence of an arbitrary static disorder potential,  $V_{dis}(x, y)$ . The classical partition function can be written as,

$$Z = \int_{w, \bar{w}} e^{\beta E[w, \bar{w}] + \beta \int d^2x V_{dis}(x, y) \rho(x, y)} \quad (5.1)$$

The spin polarization of the system (of size  $L$ ) is given by the thermal average

$$\langle SP \rangle = \frac{1}{\pi L^2} \frac{1}{4\pi} \frac{1}{Z} \int_{w, \bar{w}} \frac{1 - w\bar{w}}{1 + w\bar{w}} e^{\beta E[w, \bar{w}] + \beta \int d^2x V_{dis}(x, y) \rho(x, y)} \quad (5.2)$$

Note that at  $g = 0$ , the energy functional depends only on the charge density and is  $O(3)$  invariant. If we make the transformation of  $w' \rightarrow 1/w$ , the charge density and hence

the energy density are invariant but the spin density changes sign. Equation (5.2) then shows that the average spin polarization vanishes. However, this argument for proving that spin polarization vanishes on average is technically incorrect since the system is realised in a broken symmetry phase. Thus the average in equation (5.2) is only over configurations satisfying the boundary conditions,

$$\lim_{|z| \rightarrow \infty} w(z, \bar{z}) = w_\infty \quad (5.3)$$

where  $w_\infty$  is a fixed value. Since  $w'$  and  $w$  clearly cannot both satisfy the above condition, the above argument is flawed.

We now give a more sophisticated argument which takes into account the above point and prove the result for a large class of configurations. Without loss of generality, we can put  $w_\infty = 0$ . We first consider analytic configurations of an  $N$  skyrmion system,

$$w(z) = \sum_{n=1}^N \frac{\lambda_n}{(z - \mathbf{R}_n^{np})} \quad (5.4)$$

Where  $|\mathbf{R}_n^{np}| \leq L$  and the labelling is such that  $n > m \Rightarrow |\mathbf{R}_n^{np}| > |\mathbf{R}_m^{np}|$ . Let  $\mathbf{R}_n^{sp}$  denote the zeroes of  $w$ . The boundary condition,  $w_\infty = 0$ , ensures that atleast one of the zeroes lies at infinity.  $w$  can then be written as a product of the positions of the poles and zeros:

$$w(z) = \lambda \frac{\prod_{n=1}^{N-1} (z - \mathbf{R}_n^{sp})}{\prod_{n=1}^N (z - \mathbf{R}_n^{np})} \quad (5.5)$$

where,

$$\lambda = \sum_{n=0}^N \lambda_n \quad (5.6)$$

If  $\lambda = 0$  implies that there is more than one zero at infinity. For every such configuration, there are a very large number of nearby configurations of the type  $\lambda_n = \lambda_n + \delta\lambda_n$ , for which  $\lambda \neq 0$ . Thus the set of  $\lambda = 0$  configurations has negligible statistical weight. So for a generic analytic configuration, only one zero lies at infinity. We concentrate on these configurations and rewrite  $w$  as,

$$w(z) = \frac{\lambda}{z - \mathbf{R}_N^{np}} \prod_{n=1}^{N-1} \frac{z - \mathbf{R}_n^{sp}}{z - \mathbf{R}_n^{np}} \quad (5.7)$$

Now consider the configuration,

$$w'(z) = \frac{1}{\lambda} \frac{(\mathbf{R}_N^{np})^2}{(z - \mathbf{R}_N^{np})} \prod_{n=1}^{N-1} \frac{z - \mathbf{R}_n^{np}}{z - \mathbf{R}_n^{sp}} \quad (5.8)$$



$w'$  satisfies the boundary conditions (5.3). In the region  $|z| \ll \mathbf{R}_N^{np}$ , we have

$$\begin{aligned} w'(z) &\approx -\frac{\mathbf{R}_N^{np}}{\lambda} \prod_{n=1}^{N-1} \frac{z - \mathbf{R}_n^{np}}{z - \mathbf{R}_n^{sp}} \\ &\approx \frac{1}{w(z)} \end{aligned} \quad (5.9)$$

Thus, for every configuration  $w(z)$ , there exists another configuration  $w'(z)$  which satisfies the same boundary conditions and except in a region around one point near the edge, is equal to  $1/w(z)$ . The important fact is that the area of this region does not change as we take the thermodynamic limit,  $N, L \rightarrow \infty$ ,  $N/(\pi L^2) \rightarrow \rho$ . For short range interactions we then have,

$$\begin{aligned} E[w] &= E[w'] + o(L^0) \\ SP[w] &= -SP[w'] + o(L^0) \end{aligned} \quad (5.10)$$

Note that a  $1/r$  interaction in two dimensions is short-ranged in this sense. Equation (5.2) then shows that the average spin polarization density vanishes in the thermodynamic limit.

We now generalize this proof for arbitrary configurations that have only one zero at infinity. Consider configurations that satisfy,

$$\begin{aligned} \lim_{|z| \rightarrow \infty} w(z, \bar{z}) &= 0 \\ \lim_{|z| \rightarrow \infty} zw(z, \bar{z}) &= \lambda \end{aligned} \quad (5.11)$$

Define,

$$w'(z, \bar{z}) = \left( \frac{R_N^{np}}{z - R_N^{np}} \right)^2 \frac{1}{w(z, \bar{z})} \quad (5.12)$$

It can easily be verified that  $w'$  satisfies the boundary conditions (5.3) and that equations (5.9) and (5.10) hold true. Thus if we assume that, as has been shown for analytic configurations, the generic configuration has only one zero at infinity, we have proved that the spin polarization density will vanish in the thermodynamic limit.

## B. Spin Polarization at $g \approx 0$

The results obtained in the previous section show that for a system with  $g$  exactly zero, the spin polarization changes discontinuously from its fully polarized value at  $\nu = 1$  to zero when the filling factor changes from 1. In a real system,  $g$  will never be exactly equal to

zero but will have some very small value. Correspondingly, the single skyrmion at  $\nu = 1$  will have a large but finite size. The  $g \sim 0$  regime discussed in this paper will occur at filling factors where this size becomes comparable to the inter-skyrmion spacing, eg. in the low  $g$  experiments<sup>8,9</sup>, the single skyrmion spin at  $\nu = 1$  has been estimated to be around 30-40. As mentioned earlier, for "hedgehog" skyrmions, the spin,  $s$  can be related to the rms charge radius as  $\langle r^2 \rangle = 2s$  (see Appendix 2). Setting the inter-skyrmion spacing,  $a = \sqrt{2\pi/(1-\nu)}$  equal to the charge radius,  $\sqrt{2s}$  yields  $\nu \sim 0.9$ . Thus  $\nu \leq 0.9$  will be the  $g \approx 0$  regime for these skyrmions.

We have calculated the spin polarisation at  $g = 0.05g_0$  in both the high and low stiffness limits. The skyrmion lattice configuration that minimizes the energy now has a value of  $\lambda$  slightly away from the symmetric point resulting in a non-zero spin polarisation. The spin polarisation is calculated from

$$SP_{lattice} = \frac{\nu}{4\pi A_{\square}} \int_{\square} \frac{1 - \bar{w}w}{1 + \bar{w}w} \quad (5.13)$$

The results are plotted in Figs. 14 and 15. As can be seen they are not very different. The spin polarization falls sharply to about 10% of its  $\nu = 1$  value at  $\nu = .97$  and  $\nu = .98$  in the high and low stiffness limits respectively. Both are down to about 1% at  $\nu = 0.9$ . At this value of  $g$ , we have calculated the single skyrmion spin, as described in Appendix 1 to be 45 and 33 in the low and high stiffness limits respectively. This implies that the spin polarization has fallen to 10% when the charge radius is equal to half the inter-skyrmion spacing. i.e. when they are just touching each other. It has fallen to about 1% when the radius is roughly equal to the lattice spacing. This is consistent with our general arguments of the previous paragraph.

To summarize, we predict that the spin polarization will fall sharply to about 10% of the fully polarized value at  $\nu = 1 - (\pi/4s)$ , where  $s$  is the single skyrmion spin measured at  $\nu = 1$ . It will fall to almost zero at around  $\nu = 1 - (\pi/s)$  and remain zero as  $\nu$  decreases further.

These predictions are based on our calculations done at zero temperature and in absence of disorder. However previous work indicates that the spin polarization may be fairly insensitive to these effects. The Hartree-Fock calculation of Brey et. al.<sup>10</sup> was done for the pure system at zero temperature. Nevertheless, the calculated spin polarization (at  $g = g_0$ ) matched fairly well with the experiments of Barret et. al.<sup>5</sup> which were done at 1.55 K. Thus the

predictions in the previous paragraph may well hold for real systems.

## VI. CONCLUSIONS

In this paper we have studied the ground state configuration of a lattice of overlapping skyrmions in various stiffness regimes. Their behaviour is qualitatively different from small, well-separated skyrmions. While well-separated skyrmions can be described well by the oriented, charged disc picture, for overlapping large skyrmions this picture breaks down. A lattice of large skyrmions is described by the form of the ansatz given in Section III which is specified completely in terms of the positions and strengths of the poles and zeros. The north poles are the lattice points and the south poles determined by the parameter  $\mathbf{q}$ . In the case of Néel ordered, face-centered rectangular lattices, the south poles lie at the center of the unit cell. We then argued that there exists a special value of  $\lambda = \lambda_s$  when the charge and spin densities are symmetrically distributed around the north and south poles. In the case when the lattice was rectangular the charge density formed a smaller face-centered rectangular lattice. When the lattice was square the charge density also had the symmetry of a smaller square. In all cases the spin density was peaked in opposite directions at the north and south poles and the  $z$  component of the spin vanishes. Since this distribution corresponds to the most symmetric distribution of spin and charge we expect that this also minimises the energy.

We verify the above arguments numerically in Section IV. We find that in the high stiffness regime the underlying skyrmion lattice is Néel ordered and rectangular (with aspect ratio  $\sqrt{3}$ ) corresponding to the charge density having the symmetry of a triangular lattice. The value  $\lambda_{min}$  which minimises the energy was found to be exactly equal to the value  $\lambda_s$  at which there was complete symmetry between the north and south poles. In the low stiffness regime the underlying lattice and charge density had square symmetry. In the intermediate regimes the lattice was rectangular with an aspect ratio between  $\sqrt{3}$  and 1. In all cases the  $z$ -component of the spin vanished.

We give a general argument for the vanishing of the spin polarization at  $g = 0$  at finite temperature and in the presence of disorder. We also discuss some experimental consequences. We calculate the spin polarisation at small but non-zero  $g$ . We predict that this quantity falls sharply to 10% of the fully polarised value at  $\nu = 1 - \pi/4s$  and to almost

zero at  $\nu = 1 - \pi/s$ .

We conclude that in the regime of small Zeeman coupling, skyrmions are large and overlapping and the oriented, charged-disc picture breaks down. This is because there is a distribution of charge and spin around the south poles also unlike in the charged-disc picture where they were distributed only around the north poles. The charge and spin densities can have a higher symmetry than the underlying lattice in the overlapping case unlike in the well-separated case. The universal features of the classical ground state are (1) Néel ordered rectangular lattices of skyrmions with the charge density having the symmetry of a face-centered rectangular lattice and (2) vanishing of the  $z$ -component of the spin.

- 
- <sup>1</sup> S. L. Sondhi, A. Karlhede, S. A. Kivelson and E. H. Rezayi, Phys. Rev. **B47**, 16419 (1993).
  - <sup>2</sup> D. H. Lee and C. L. Kane, Phys. Rev. Lett. **64**, 1313 (1990).
  - <sup>3</sup> H. A. Fertig, L. Brey, R. Côté and A. H. MacDonald, Phys. Rev. **B50**, 11018 (1994) ; K. Moon, H. Mori, K. Yang, S. M. Girvin, A. H. MacDonald, L. Zheng, D. Yoshioka and S. C. Zhang, *ibid.* **51**, 5138 (1995).
  - <sup>4</sup> H. A. Fertig, Luis Brey, R. Côté, A. H. Macdonald, A. Karlhede and S. L. Sondhi, Phys. Rev. **B55**, 10671 (1997).
  - <sup>5</sup> S. E. Barrett, G. Dabbagh, L. N. Pfeiffer, K. W. West and R. Tycko, Phys. Rev. Lett. **74**, 5112 (1995) ; S. E. Barrett, G. Dabbagh, L. N. Pfeiffer, K. W. West, and R. Tycko, Phys. Rev. Lett. **72**, 1368 (1994) ; R. Tycko, S. E. Barrett, G. Dabbagh, L. N. Pfeiffer and K. W. West, Science **268**, 1460 (1995).
  - <sup>6</sup> E. H. Aifer, B. B. Goldberg and D. A. Broido, Phys. Rev. Lett. **76**, 680 (1996).
  - <sup>7</sup> A. Schmeller, J. P. Eisenstein, L. N. Pfeiffer and K. W. West, Phys. Rev. Lett. **75**, 4290 (1995).
  - <sup>8</sup> S. P. Shukla, M. Shayagan, S. P. Parihar, S. A. Lyon, N. R. Cooper and A. A. Kiselev, Phys. Rev. **B61**, 4469 (2000).
  - <sup>9</sup> D. R. Leadley, R. J. Nicholas, D. K. Maude, A. N. Utjuzh, J. C. Portal, J. J. Harris and C. T. Foxon, Semicond. Sci. Technol. **13**, 671 (1998).
  - <sup>10</sup> L. Brey, H.A. Fertig, R.Côté and A. H. Macdonald, Phys. Rev. Lett **75**, 2562 (1995).
  - <sup>11</sup> A. G. Green, I.I. Kogan and A. M. Tsevelik, Phys. Rev. **B54**, 16398 (1996).
  - <sup>12</sup> Madan Rao, Surajit Sengupta and R. Shankar, Phys. Rev. Lett **79**, 3998 (1997).

- <sup>13</sup> Carsten Timm, S. M. Girvin and H. A. Fertig, Phys. Rev. **B58**, 10634 (1998).
- <sup>14</sup> R. Côté, A. H. MacDonald, L. Brey, H. A. Fertig, S. M. Girvin and H. T. C. Stoof, Phys. Rev. Lett. **78**, 4825 (1995).
- <sup>15</sup> K. Moon and K. Mullen, Phys. Rev. **B 57**, 14833 (1998); K. Moon and K. Mullen, Phys. Rev. Lett. **84**, 975 (2000).
- <sup>16</sup> H. A. Fertig, L. Brey, R. Côté, A. H. Mac Donald, A. Karlhede and S. L. Sondhi, Phys. Rev. **B55**, 10671 (1997).
- <sup>17</sup> A. A. Belavin and A. M. Polyakov, JETP Lett. **22**, 245 (1975).
- <sup>18</sup> I. V. Kukushkin, K. v. Klitzing and K. Eberl, Phys. Rev. **B55**, 10607 (1997).
- <sup>19</sup> V. Bayot, E. Grivei, S. Melinte, M. B. Santos and M. Shayegan, Phys. Rev. Lett. **76**, 4584; V. Bayot, E. Grivei, J.-M. Beuken, S. Melinte and M. Shayegan, **79**, 1718 (1997).
- <sup>20</sup> Charge density plots in color are available from the authors on request.

## Appendix 1

In this appendix we calculate the scaling form of the single skyrmion energies with the parameter  $\lambda$  and also the spin polarisation of a lattice of such skyrmions. The ansatz chosen to minimize the energy of a single skyrmion with winding number 1 at  $g = 0$  is of the form

$$w(z) = \frac{\lambda}{r} e^{-\kappa r} \quad (6.1)$$

The ansatz is not analytic anymore and has an exponential damping factor. From the form of the individual energies given in the previous sections we can see that they scale with  $\lambda$  as

$$\begin{aligned} E_{grn}(\kappa, \lambda) &= E_{grn}(\kappa, 1) \\ E_z(\kappa, \lambda) &= \lambda^2 E_z(\kappa, 1) \\ E_{coul}(\kappa, \lambda) &= \frac{1}{\lambda} E_{coul}(\kappa, 1) \end{aligned} \quad (6.2)$$

From this scaling relation we can calculate the  $\lambda$  which minimizes the energy

$$\lambda_{min}^3 = \frac{E_c(\kappa, 1)}{2E_z(\kappa, 1)} \quad (6.3)$$

Therefore the minimum energy is

$$E(\kappa, \lambda_{min}) = E_{grn}(\kappa, 1) + \lambda_{min}^2 E_z(\kappa, 1) + \frac{1}{\lambda_{min}} E_{coul}(\kappa, 1) \quad (6.4)$$

The excess spin per skyrmion corresponding to the minimum configuration is

$$spin = \lambda_{min}^2 \frac{1}{2\pi} \int \frac{\bar{w}w}{1 + \bar{w}w} \quad (6.5)$$

To extract the spin polarisation of a collection of well separated  $N_{sky}$  number of single skyrmions we have to sum over all the individual spins and subtract out the spin of the vacuum state ( $spin_{vac}$ ). Thus,

$$\begin{aligned} spin_{DL} &= N_{sky} spin - spin_{vac} \\ \frac{spin_{DL}}{A} &= \frac{spin}{A_{\square}} - \frac{\nu}{4\pi} \\ &= \frac{1}{2\pi} ((1 - \nu)spin - \frac{\nu}{2}) \end{aligned} \quad (6.6)$$

where  $A$  is the area of the sample and  $A_{\square}$  is the area of the unit cell of the dilute lattice formed by the skyrmions.

## Appendix 2

In this appendix we show the relation between the spin  $s$  of a hedgehog skyrmion and its rms charge radius  $r$  i.e.  $\langle r^2 \rangle = 2s$ . Consider a single skyrmion described by the ansatz

$$w(z) = \frac{F(r)}{z} \quad (6.7)$$

where  $r$  is the rms charge radius and  $F(r)$  is an analytic function of the rms charge radius. The spin of this skyrmion is

$$s = \frac{1}{2\pi} \int \frac{F^2 d^2r}{r^2 + F^2} \quad (6.8)$$

Its charge density is

$$\begin{aligned} \rho(r) &= \frac{1}{2\pi i} \frac{\epsilon_{ij} \partial_i \bar{w} \partial_j w}{(1 + \bar{w}w)^2} \\ &= \frac{1}{2\pi i} \partial_i \frac{\epsilon_{ij} \bar{w} \partial_j w}{(1 + \bar{w}w)} \end{aligned} \quad (6.9)$$

Now,

$$\begin{aligned} \langle r^2 \rangle &= \int r^2 \rho(r) d^2r \\ &= \frac{\epsilon_{ij}}{2\pi i} \int r^2 \partial_i \frac{\bar{w} \partial_j w}{(1 + \bar{w}w)} \\ &= -\frac{\epsilon_{ij}}{2\pi i} \int \frac{2r_i \bar{w} \partial_j w}{(1 + \bar{w}w)} \end{aligned} \quad (6.10)$$

Using,

$$\begin{aligned}\partial_j w &= \frac{F' r_j}{zr} + F \partial_j (1/z) \\ i.e \quad \partial_x w &= -\frac{w}{z} \quad \& \\ \partial_y w &= -\frac{iw}{z}\end{aligned}\tag{6.11}$$

we get

$$\langle r^2 \rangle = 2s \tag{6.12}$$

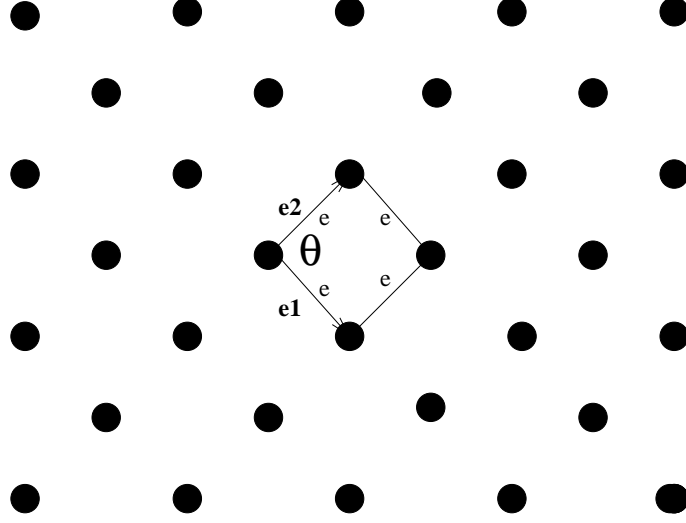


Fig. 1. The face-centered rectangular lattice with basis vectors

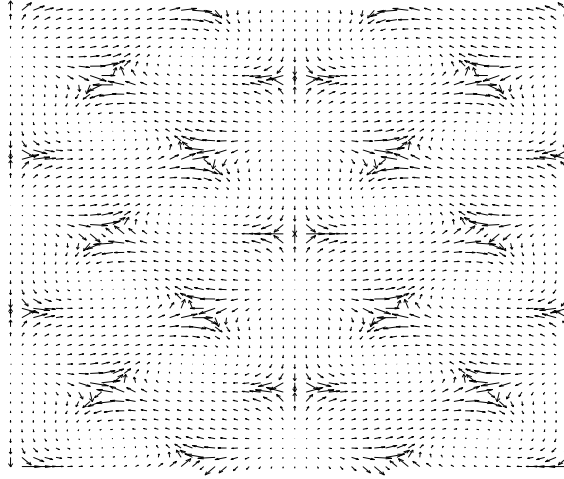


Fig. 2. XY spin configuration in a triangular lattice of well separated skyrmions

$$(\mathbf{q} = (2\pi/3, 2\pi/3)).$$



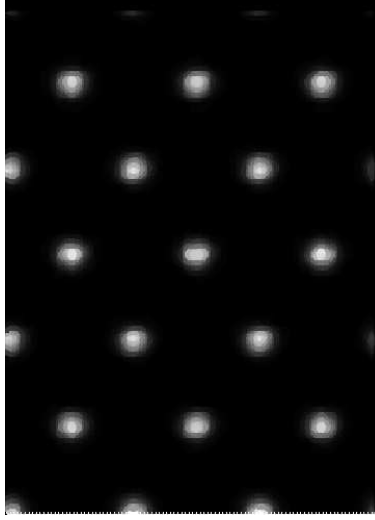


Fig. 3. Charge density profile in a triangular lattice of well separated skyrmions. The higher values are shaded in white.

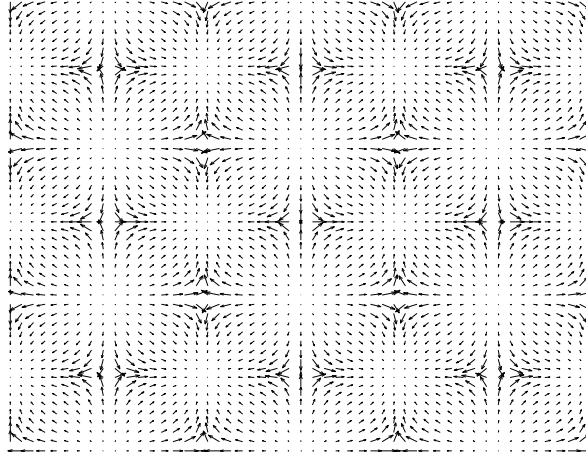


Fig. 4. XY spin configuration in a square lattice of well separated skyrmions ( $\mathbf{q} = (\pi, \pi)$ ).

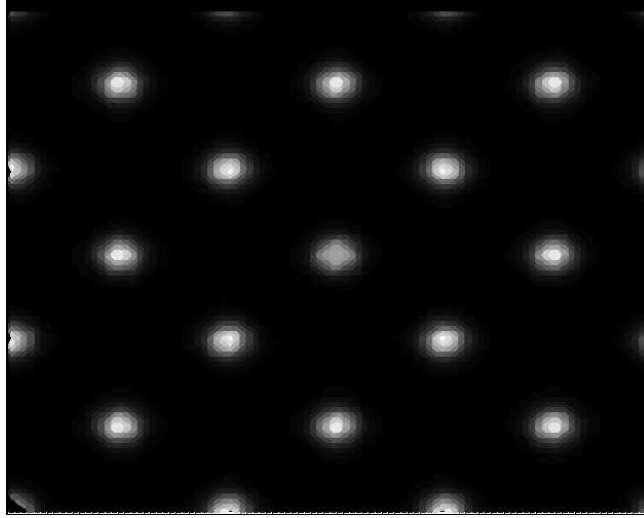


Fig. 5. Charge density profile in a square lattice of well separated skyrmions. The higher values are shaded in white.

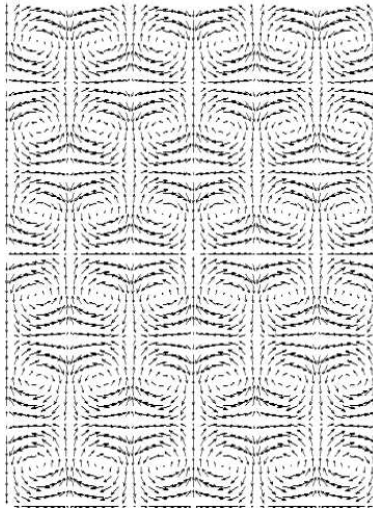


Fig. 6. XY spin configuration in a Néel ordered, rectangular lattice of overlapping skyrmions.

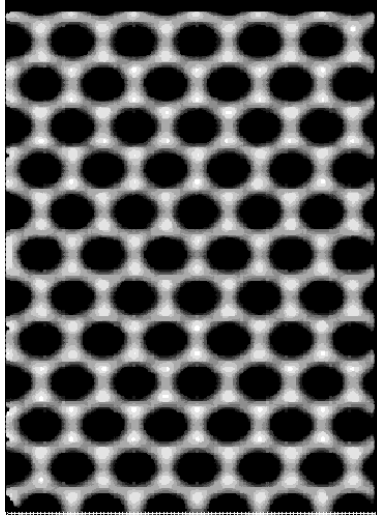


Fig. 7. Charge density profile in a Néel ordered, rectangular lattice of overlapping skyrmions.  
The higher values are shaded in white.

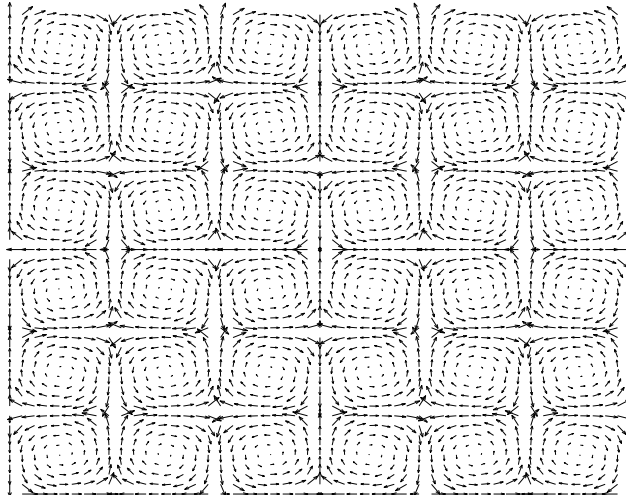


Fig. 8. XY spin configuration in a Néel ordered, square lattice of overlapping skyrmions.

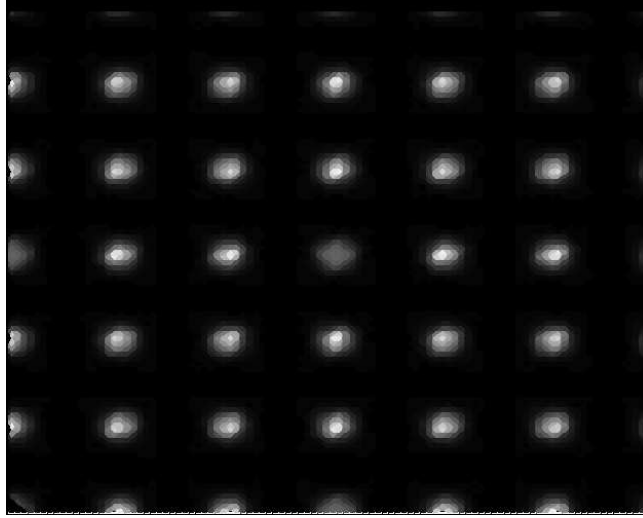


Fig. 9. Charge density profile in a Néel ordered, square lattice of overlapping skyrmions. The higher values are shaded in white.

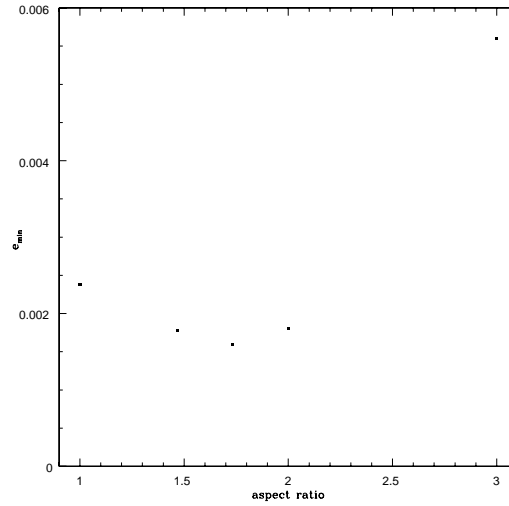


Fig. 10. Plot of the value of minimized energy (with respect to  $\lambda$  and  $q$ ). Notice that the minimum occurs when the aspect ratio has value  $\sqrt{3}$ .

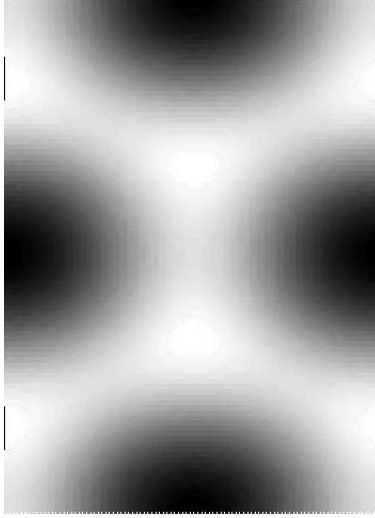


Fig. 11. Charge density profile in the unit cell of the rectangular lattice (aspect ratio  $\sqrt{3}$ ) at  $\nu = 0.90$ , in the high stiffness limit.

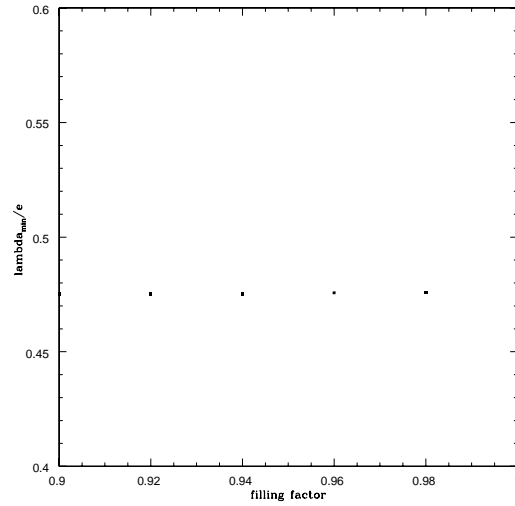


Fig. 12. Scaling of  $\lambda$  with the lattice size paramter  $e$  as a function of the filling factor in the high stiffness regime. A similar graph is obtained in the low stiffness regime also.

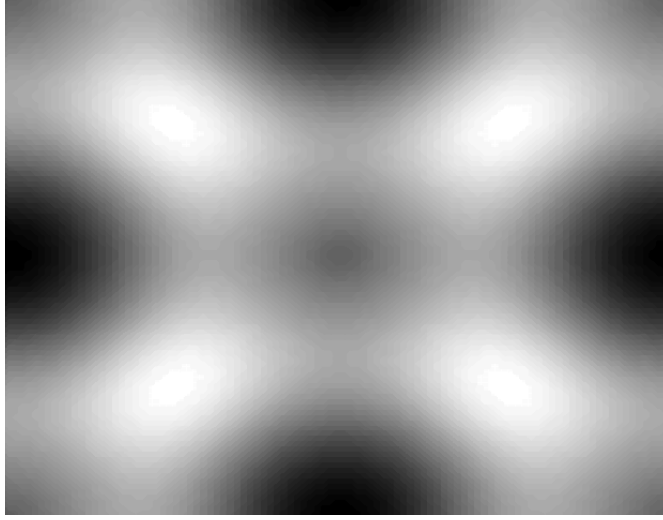


Fig. 13. Charge density profile in the square unit cell in the low stiffness limit at  $\nu = 0.98$ .

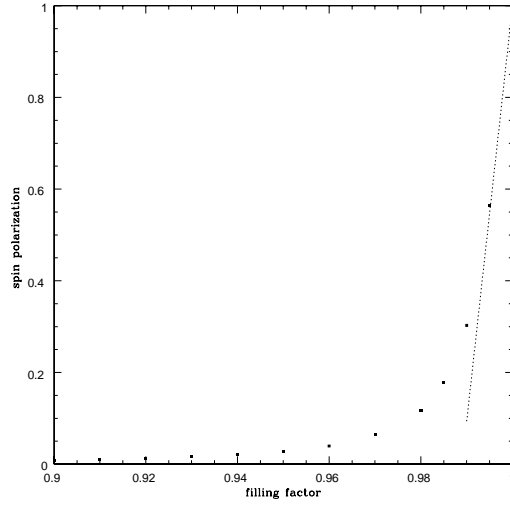


Fig. 14. Plot of the value of the spin polarization as a function of the filling factor in the high stiffness regime. The dotted line is the curve calculated from a dilute lattice of isolated skyrmions.

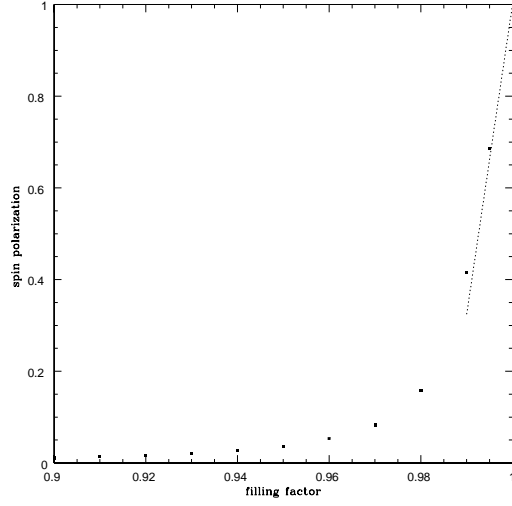


Fig. 15. Plot of the value of the spin polarization as a function of the filling factor in the low stiffness regime. The dotted line is the curve calculated from a dilute lattice of isolated skyrmions.